Precision of the Chinese Space Station Telescope (CSST) stellar radial velocities

Yang Sun, Ding-Shan Deng and Hai-Bo Yuan

Department of Astronomy, Beijing Normal University, Beijing 100875, China; *yuanhb@bnu.edu.cn*

Abstract The Chinese Space Station Telescope (CSST) spectroscopic survey plans to deliver high-quality low-resolution ($R > 200$) slitless spectra for hundreds of millions of targets down to a limiting magnitude of about 21 mag, covering a large survey area ($17\,500 \deg^2$) and a wide wavelength range (255–1000 nm by three bands GU, GV, and GI). In this work, we use empirical spectra of the Next Generation Spectral Library to simulate the CSST stellar spectra at $R = 250$, and investigate their capabilities in measuring radial velocities. We find that velocity uncertainties depend strongly on effective temperature, weakly on metallicity for only FGK stars, and hardly on surface gravity. It is possible to deliver stellar radial velocities to a precision of about $3\,\mathrm{km\,s^{-1}}$ for AFGKM stars, and about $10\,\mathrm{km\,s^{-1}}$ for OB stars, at signal-to-noise ratio (SNR) of 100. Velocity uncertainties using single GU/GV/GI band spectra are also explored. Given the same SNR, the GU band performs best, the GV band the second best, and then the GI band. The effects of spectral normalization and the imperfect template on velocity measurements are investigated and found to be very weak. The uncertainties caused by wavelength calibration are considered and found to be moderate. Given the possible precision of radial velocities, the CSST spectroscopic survey can enable interesting science such as searching for hyper-velocity stars. Limitations of our results are also discussed.

Key words: methods: data analysis — methods: statistical — stars: fundamental parameters — stars: kinematics and dynamics

1 INTRODUCTION

The Chinese Space Station Telescope (CSST) optical survey (CSS-OS; Zhan 2011, 2018; Cao et al. 2018; Gong et al. 2019) is one of the leading astronomical projects in China. With the CSST, a 2-meter space telescope of a large field of view of $1.1 \deg^2$ and sharing the same orbit of the Chinese Space Station, it will simultaneously carry out both photometric and slitless grating spectroscopic surveys, covering a large sky area of $17\,500 \deg^2$ but at a high spatial resolution of $\sim 0.15''$ in about ten years. The imaging survey has seven photometric filters, i.e., NUV, u, g, r, i, z, and y bands, covering 255–1000 nm from the near-ultraviolet (NUV) to near infrared (NIR). Meanwhile, the slitless spectroscopic survey has three bands, GU (255–420 nm), GV (400–650 nm), and GI (620–1000 nm), at a spectral resolving power larger than 200. The main scientific goals of the CCS-OS include the nature of dark matter and dark energy, large scale structure and cosmology, galaxy formation and evolution, active

galactic nuclei (AGNs), the Milky Way and near-field cosmology, stellar physics, solar system, and astrometry.

Given the very low sky background and very high spatial resolution, space-based wide-field slitless spectroscopic surveys are very powerful tools in astronomy (Glazebrook et al. 2005). Complementary to the CSST imaging survey, the CSST spectroscopic survey aims to deliver high-quality slitless spectra covering 250–1000 nm at R larger than 200 for hundreds of millions of stars and galaxies. Such a large and magnitude-limited sample of stars will provide a great opportunity for studies of stars and the Galaxy. However, precise stellar parameters have to be extracted from the unique CSST low resolution spectra first. It is shown that (Ting et al. 2017) stellar parameters (e.g., effective temperatures, surface gravities and elemental abundances) can be determined almost to the same precision for different spectral resolutions ($R > 1000$), given perfect spectral models, spectral normalization, the same exposure time and the number of detector pixels. At lower resolutions, estimates of some stellar parameters may be strongly
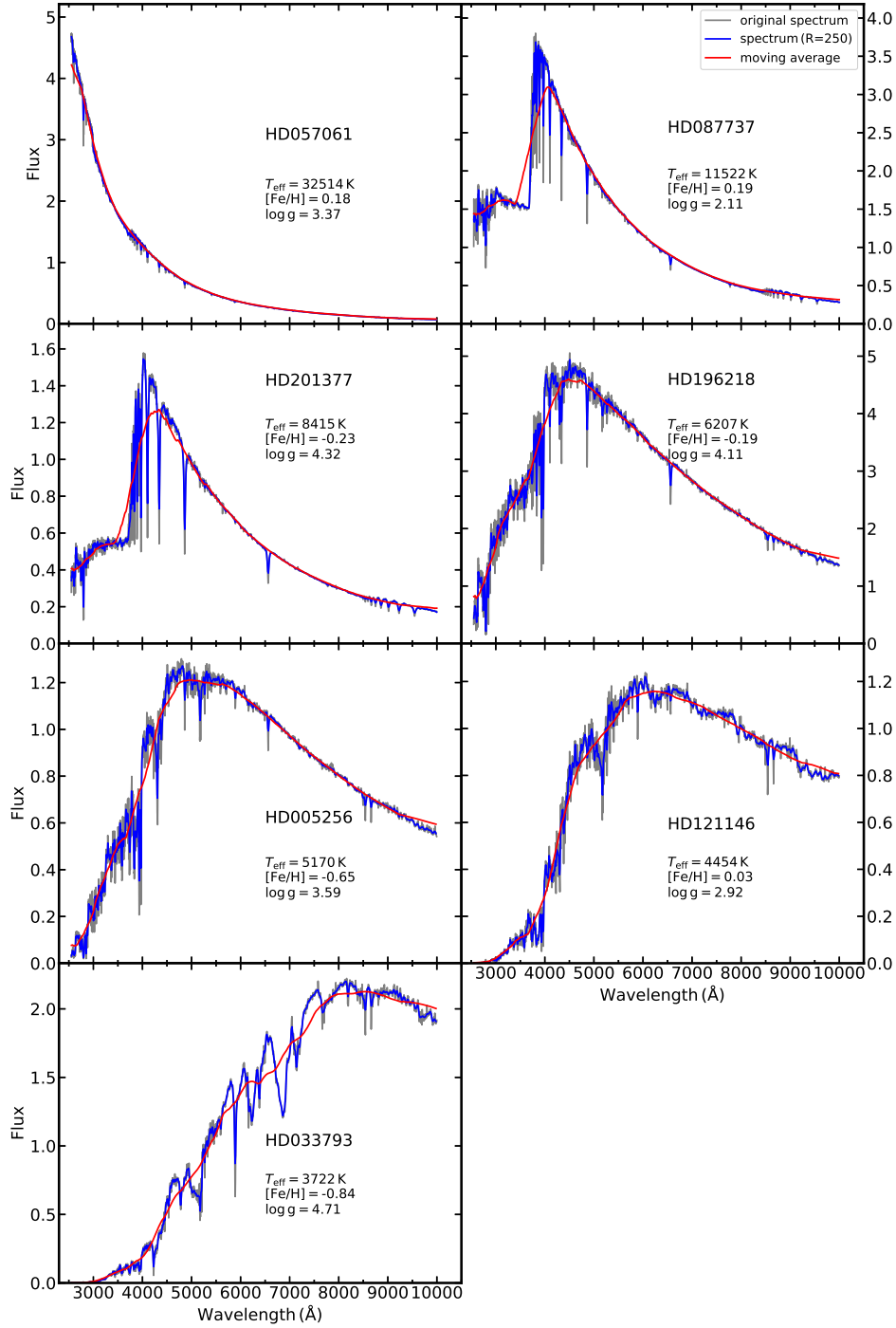
Fig. 1 NGSL spectra of representative stars of different spectral types. The Y-axes are in arbitrary units. Stellar ID and parameters are marked for each target. The *grey* and *blue lines* denote the original and degraded ($R = 250$) spectra, respectively. The *red lines* are the continua of the degraded spectra.

correlated with one another. Therefore, it is very essential to explore capabilities of the unique CSS-OS slitless spectra in deriving stellar parameters. Considering the relative simplicity in measuring radial velocities, we focus on stellar radial velocities in this paper and leave other parameters in future work.

In this work, we estimate the precision of radial velocity measurements from CSS-OS stellar spectra. Spectra from the Next Generation Spectral Library (NGSL; Heap & Lindler 2007) are used to simulate the CSS-OS spectra. A cross-correlation function (CCF) method (Baranne et al. 1996) is used to measure radial velocities, and Monte Carlo
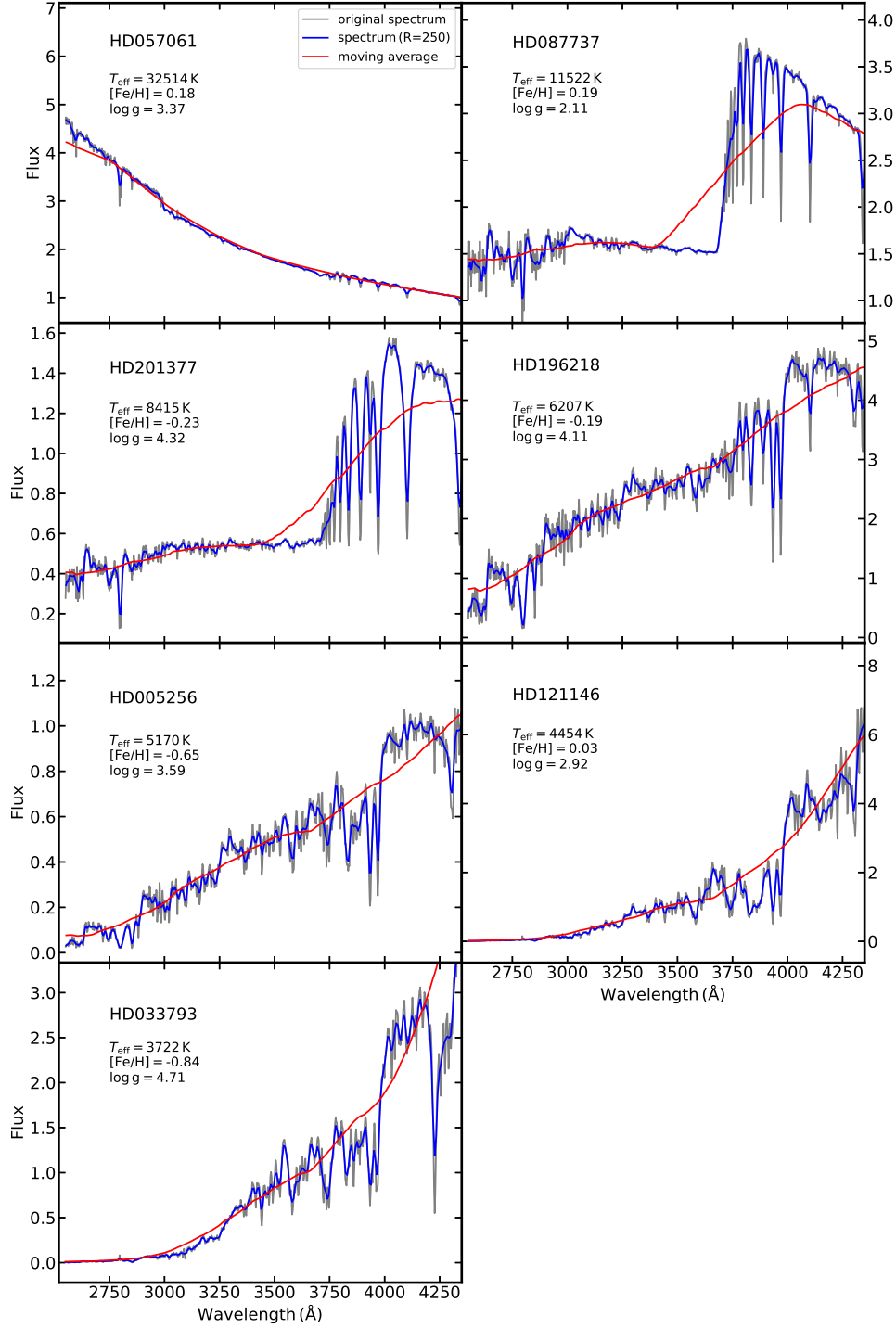
Fig. 2 Same to Fig. 1 but for the GU band spectra only.

simulations are used to compute their errors. Variations of precision of radial velocities as functions of stars' atmospheric parameters are also investigated. The paper is organized as follows. We introduce our data and method in Sections 2 and 3, respectively. The results are shown in Section 4. In Section 5, we discuss implications and limitations of our results. We conclude in Section 6.

2 DATA

In this work, we use spectra from the NGSL (Heap & Lindler 2007; Koleva & Vazdekis 2012) to simulate the CSS-OS slitless spectroscopic observations. The NGSL is an empirical stellar spectral library constructed by an HST/STIS snapshot program with the three gratings

G230LB+G430L+G750L. It contains intermediate resolution ($R \sim 1000$), UV-optical spectra (1670–10250 Å) of 378 stars spanning a wide range in temperature, luminosity, and metallicity. The spectra in this library are well calibrated and have typical SNRs of 200, 600, and 400 per pixel for the GU, GV and GI bands, respectively. Due to the good match in wavelength coverage and wide coverage in stellar types, the NGSL provides an ideal empirical dataset for the purpose of this work.

The NGSL spectra have a higher spectral resolution than the CSS-OS slitless spectra ($R > 200$). They are degraded to $R = 250$ using a Gaussian convolution method. Here we adopt a constant spectral resolution of $R = 250$ and a sampling rate of 3 pixels per resolution element for the CSS-OS spectra. Figures 1 and 2 show the comparison between the original ($R \sim 1000$) and degraded ($R = 250$) NGSL spectra for stars of different spectral types. Strong or broad stellar absorption features, such as Balmer jump (BJ), Balmer lines, Paschen lines, the D4000 break, Mg II doublet at 2800 Å, Mg I at 2852 Å, the Mg break at ~ 2600 Å, the CH G bands at 4300 Å, MgH at 5150 Å, Na I D1 and D2 lines, Ca II H&K lines, Ca II IR triplets and TiO bands, are still clearly visible in the degraded spectra. Weak and narrow absorption lines are mixed and hardly seen.

3 METHOD

We use the CCF method to measure stellar radial velocities and Monte Carlo simulations to estimate their errors. We assume that the degraded NGSL spectra have zero noises and are used as templates. For each target from the NGSL, 1000 simulated spectra for a given SNR are obtained by adding random noises to each pixel of its degraded spectrum. We then measure velocities by a Gaussian fit to the CCF of the simulated spectra with its template spectrum (Baranne et al. 1996). Dispersion value of its 1000 velocity measurements is then calculated to represent its velocity precision (σ_{RV}) at the given SNR. For a given spectrum, σ_{RV} is inversely proportional to its SNR (Fig. 3). Therefore, only one single SNR of 100 is adopted in the work. Note here the SNR refers to SNR per pixel at a sampling rate of 3 pixels per resolution element.

In the above procedure, we have assumed that all CSS-OS slitless spectra are accurately flux calibrated and reddening corrected, only then simulated spectra can be directly compared to templates without normalization. We believe that we can achieve ~ 1 per cent flux calibration for the CSS-OS slitless spectroscopic survey, with an innovative technique that uses tens of millions of stars as flux standards (Yuan et al. to be submitted). Reddening correction is relatively easy due to the fact that the CSS-OS will mostly target high Galactic latitude regions by
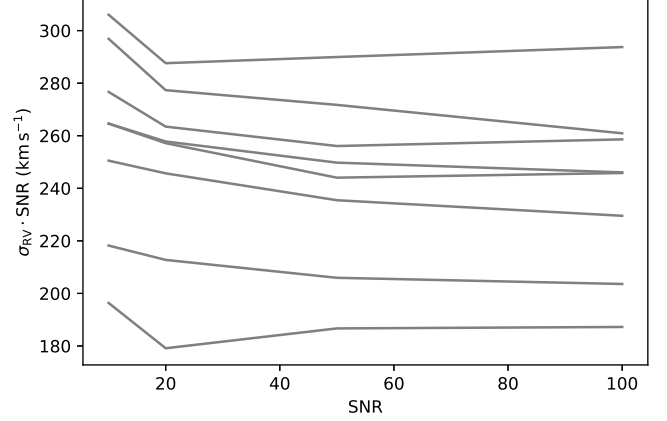

Fig. 3 The inverse relationship between σ_{RV} and SNR for eight randomly selected stars of different spectral types.

using the popular two-dimensional dust extinction maps (Schlegel et al. 1998; Planck Collaboration et al. 2014; Irfan et al. 2019; Sun et al. in prep). In cases of bad flux calibration or difficult reddening correction, observed spectra have to be normalized first to measure their velocities. Therefore, we also explore velocity precision using normalized CSS-OS spectra in the work.

However, it is non-trivial to do spectral normalization due to difficulties in defining clean continuum areas, particularly in the cases of very low spectral resolution. We adopt a simple moving average method to estimate the continuum of each spectrum, with a window size of 51 pixels. In cases of boundary pixels, where there are less than 25 pixels in one side, all pixels in that side are used. Despite its simplicity, this approach is robust, easy to be implemented and retains most features. Figures 1 and 2 show the obtained continua for representative stars of different spectral types.

The CSS-OS slitless spectrograph has three filters, GU (255–420 nm), GV (400–650 nm), and GI (620–1000 nm). For a given target, the three filters will be observed at different epochs. It means that only one segment of spectrum (GU/GV/GI) will be available in the early stage of the survey. Therefore, we also explore velocity precision using only one segment of CSS-OS spectra in the work.

4 RESULTS

4.1 Based on the Whole Spectra

We first investigate velocity uncertainties (σ_{RV}) with the full range of spectra at SNR=100. The upper-left panel of Figure 4 plots the relationship between σ_{RV} and stellar parameters (T_{eff}, [Fe/H] and $\log g$). The triangles and circles denote dwarfs ($\log g \geq 3.5$ dex) and giants ($\log g < 3.5$ dex), respectively. It can be seen that σ_{RV} depends strongly on spectral types. The σ_{RV} values are about $2 -$
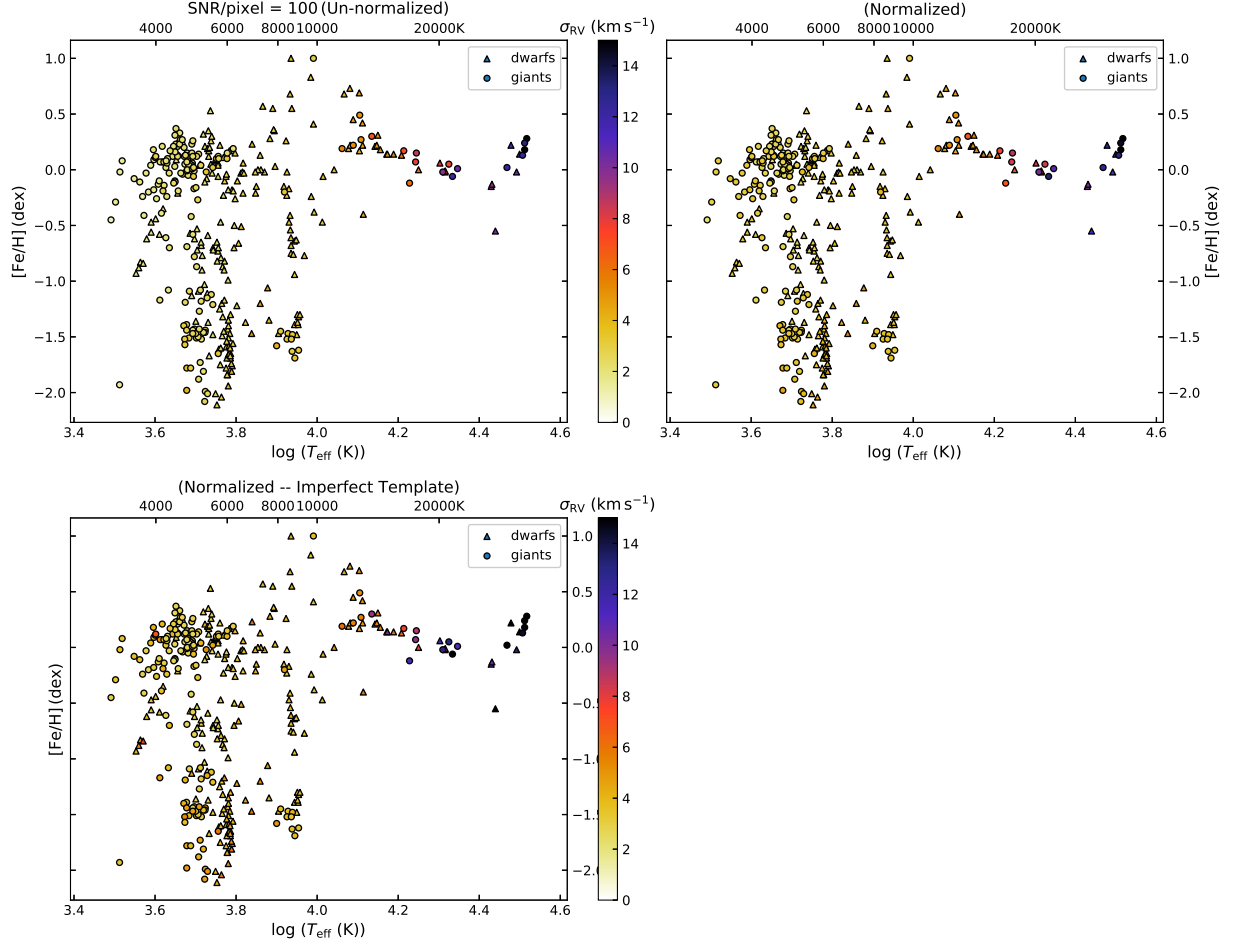
Fig. 4 The relationship between σ_{RV} and stellar parameters at SNR=100 for the un-normalized spectra (*upper-left*), the normalized spectra (*upper-right*), and the normalized spectra using the closest spectrum as a template (*lower-left*). The *triangles* and *circles* denote dwarfs and giants, respectively. The *color bar* represents the values of σ_{RV}.
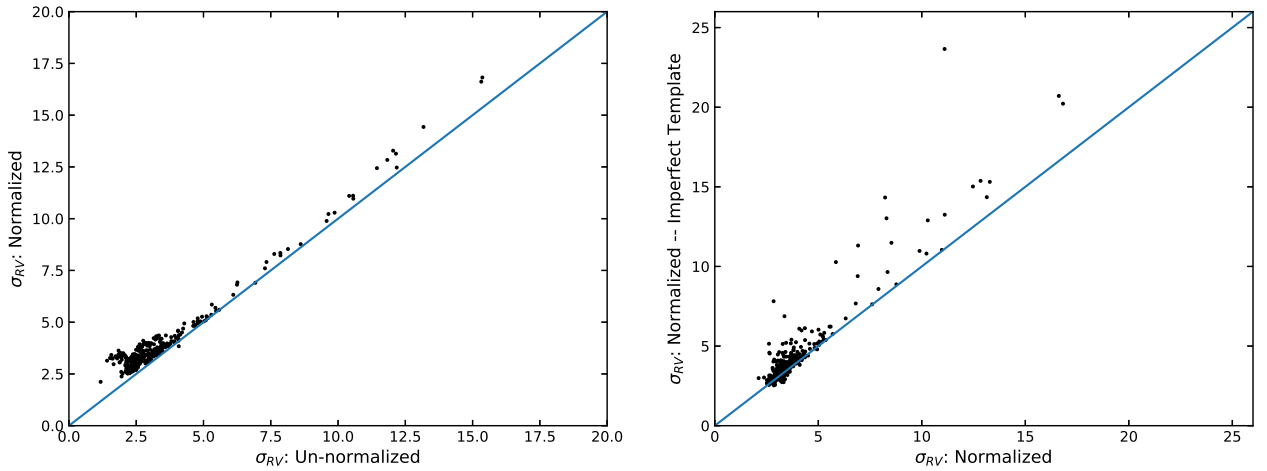

Fig. 5 Comparisons of σ_{RV} results obtained by different methods. The *blue solid line* in each panel represents the line of equality.

Table 1 Predicted Uncertainties of the CSST Stellar Radial Velocities as a Function of Effective Temperature at SNR $= 100$

T_{eff} (K)	σ_{RV} (km s^{-1})											
	un-normalized				normalized				normalized^a			
	GU	GV	GI	All	GU	GV	GI	All	GU	GV	GI	All
3250	1.8	3.3	7.1	1.6	3.7	3.7	7.7	3.3	3.7	4.5	8.4	3.5
3750	2.1	6.1	18.9	1.9	3.5	6.9	18.6	3.3	3.6	7.9	22.7	3.6
4250	2.2	7.6	24.7	2.2	3.1	8.2	25.4	3.0	3.3	8.3	26.5	3.1
4750	2.4	10.2	30.3	2.3	3.0	10.4	30.6	2.8	3.1	10.9	33.3	2.9
5250	2.5	13.0	35.0	2.5	3.2	13.9	35.4	3.0	3.2	14.9	45.0	3.1
5750	2.7	16.4	31.4	2.6	3.4	16.5	32.5	3.2	3.4	18.8	39.6	3.3
6250	3.1	15.8	28.0	3.0	4.0	15.9	30.1	4.0	4.1	17.0	38.1	4.0
6750	3.3	12.3	23.0	3.2	3.8	12.5	24.5	3.6	3.9	13.1	27.3	3.8
7250	3.5	9.5	17.1	3.3	4.0	9.7	17.9	3.7	4.3	9.8	19.6	4.0
7750	3.6	7.7	13.8	3.2	4.0	8.5	14.0	3.6	4.2	8.3	15.9	3.8
8250	3.9	6.7	11.3	3.4	4.2	7.0	12.0	3.7	4.4	7.0	12.1	3.8
8750	3.9	6.0	10.5	3.3	4.2	6.5	10.8	3.6	4.3	6.5	10.8	3.7
9250	3.8	5.8	10.3	3.2	4.2	6.1	10.4	3.5	4.1	6.2	10.6	3.6
9750	3.8	6.0	10.0	3.3	4.2	6.3	10.0	3.4	4.3	6.8	10.1	3.8
11000	4.8	7.2	11.2	4.0	5.2	7.5	11.5	4.2	5.1	7.8	11.9	4.3
13000	5.7	8.7	12.7	4.7	5.9	9.2	13.3	5.0	5.9	8.8	13.1	5.1
15000	6.4	9.6	13.9	5.3	6.6	9.8	14.2	5.5	6.7	10.2	20.0	5.7
17000	8.7	14.4	16.6	6.8	9.1	14.8	17.8	7.3	9.6	16.0	20.8	8.3
19000^b												
21000	10.8	16.0	20.3	8.0	11.0	16.8	21.8	8.4	13.2	20.2	31.7	13.0
23000	13.3	18.3	22.5	10.6	14.3	19.3	25.0	11.0	14.0	18.8	26.0	11.0
25000^b												
27000	12.6	15.8	22.7	9.6	13.1	17.3	24.2	10.2	13.5	17.8	28.2	11.0
29000	15.8	22.6	27.3	12.2	16.1	23.1	28.2	12.5	19.6	25.8	30.4	15.0
31000	16.5	18.1	26.3	11.4	16.6	18.9	27.9	12.4	19.1	24.9	36.5	15.4
33000	19.7	24.9	25.5	14.2	21.0	26.1	29.0	15.5	24.3	31.1	49.2	20.5

^{a}The closest spectrum rather than itself is used as a template. ^{b}The null values mean that there are no sample stars in these T_{eff} ranges.

$4\,\mathrm{km\,s^{-1}}$ for AFGKM stars, increase to $4 - 15\,\mathrm{km\,s^{-1}}$ for hot OB stars. There is a weak anti-correlation between [Fe/H] and σ_{RV} for FGK stars, as more metal-rich stars display stronger metal absorption lines. While $\log \mathrm{g}$ has no effects on σ_{RV}. The upper-right panel of Figure 4 shows the result from normalized spectra. The trends are very similar, but with slightly larger σ_{RV} values due to loss of information in the normalization process. The upper panels of Figure 5 compare the results between unnormalized spectra and normalized spectra. The uncertainties are only slightly larger with normalized spectra, suggesting that the effects of spectral normalization on velocity measurements are weak.

4.2 Based on GU/GV/GI Band Spectra

We also investigate velocity uncertainties using each segment of CSS-OS spectra. Figure 6 plots σ_{RV} as a function of T_{eff}, using spectra from the GI (red dots), GV (green dots), GU (blue dots) bands and the whole spectra (black dots). Similarly, the upper-left, upper-right, and lower-left panels show results from the un-normalized spectra, the normalized spectra, and the normalized spectra using the closest spectrum as template, respectively. We divide the sample into different T_{eff} bins. The bin size is $500\,\mathrm{K}$ for T_{eff} from 3000 to $10\,000\,\mathrm{K}$, and is $2000\,\mathrm{K}$ for

hotter stars. The median values of σ_{RV} are estimated for each bin and listed in Table 1.

The upper-left panel of Figure 6 shows that the GU band plays a key role in measuring stellar radial velocities. At the same SNR, $\sigma_{\mathrm{RV(GU)}} < \sigma_{\mathrm{RV(GV)}} < \sigma_{\mathrm{RV(GI)}}$ for all types of stars, due to more absorption features in the blue. But note in real cases, due to the usually lower SNRs of the GU band spectra than those of the GV and GI bands, the precision of velocity measurements would not be determined by the GU band. All the three bands shall play different roles in measuring velocities. σ_{RV} depends strongly on T_{eff}. For the GI band, $\sigma_{\mathrm{RV(GI)}}$ is lowest, about $7\,\mathrm{km\,s^{-1}}$, for very cool stars due to strong molecular absorption bands in the spectra. Then the values increase rapidly to about $30\,\mathrm{km\,s^{-1}}$ at T_{eff} around 4500 K, then decrease slowly to about $10\,\mathrm{km\,s^{-1}}$ at T_{eff} around $10\,000$ K due to stronger Balmer lines and increase again to about $25\,\mathrm{km\,s^{-1}}$ at T_{eff} around 33 000 K. The large scattering around FGK stars is caused by different metallicities. For the GV band, it shows the similar trend with the GI band. It performs best both for cool M stars (about $4\,\mathrm{km\,s^{-1}}$) due to strong molecular absorption bands and for A stars (about $6\,\mathrm{km\,s^{-1}}$) due to strong Balmer lines. Thanks to different strong features for different types of stars in the GU band, such as Balmer lines and BJ for hot stars, Mg II doublet at 2800Å, Ca H&K lines and D4000 break for cool stars,
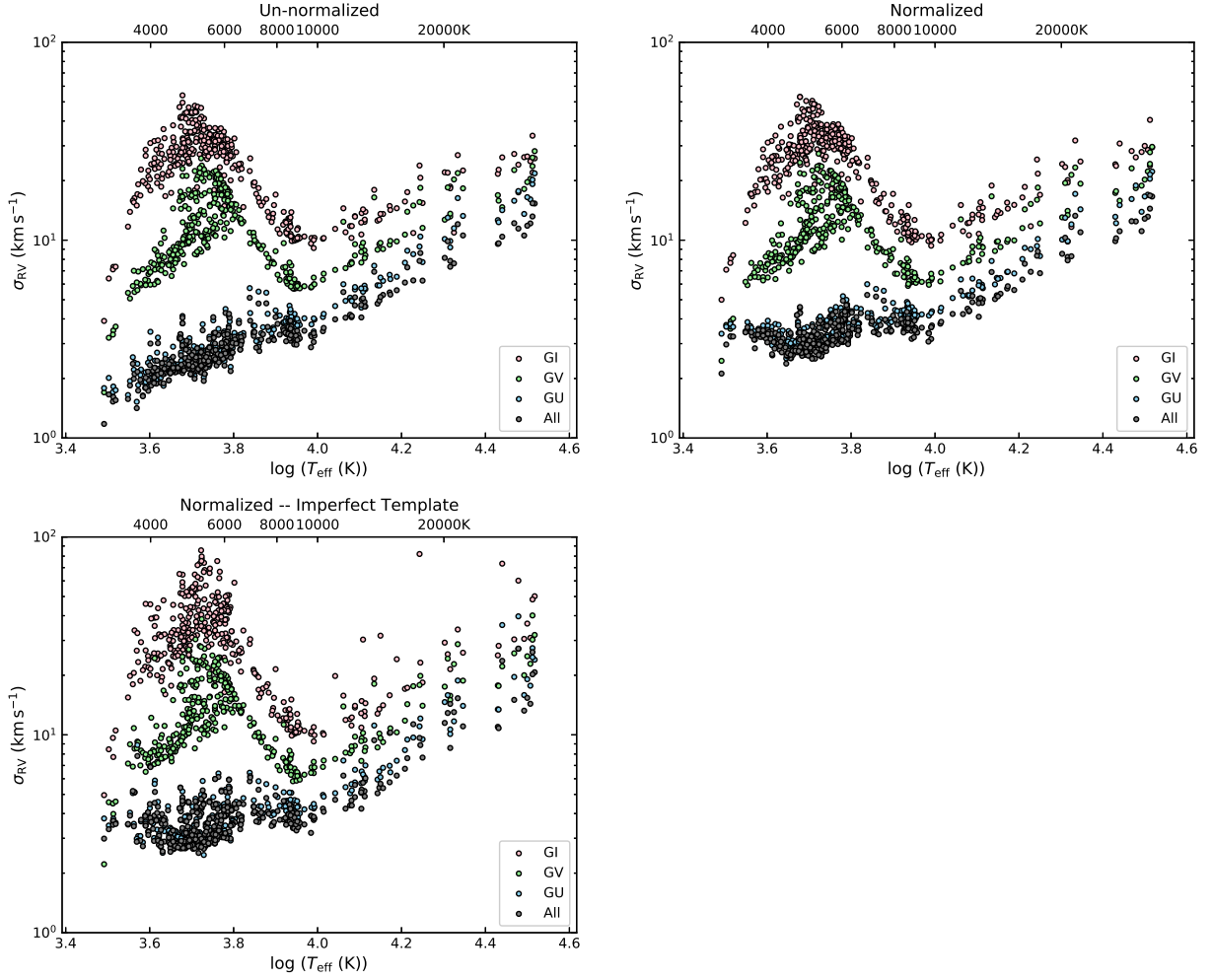
Fig. 6 The relationship between σ_{RV} and T_{eff} at SNR=100 for the un-normalized spectra (*upper-left*), the normalized spectra (*upper-right*), and the normalized spectra and the closest spectrum as template (*lower-left*). The *red, green, blue* and *black dots* represent results measured using the GI, GV, GU, and the full spectra, respectively.

$\sigma_{RV(GU)}$ increases almost monotonically with T_{eff}, from $2\,\mathrm{km\,s^{-1}}$ for M stars to $20\,\mathrm{km\,s^{-1}}$ for O stars. The upper-right and lower-left panels in Figure 6 show similar trends.

Note that eight stars, HD190073, GL109, LHS10, LHS482, G 260-36, CD-691618, HD188262 and HD193495, are excluded in the above analysis. For the first six sources, their spectra in the GU band are noisy due to low SNRs. For HD193495 and HD188262, their GU band spectra show much higher fluxes at 2550–3000 Å than expected.

5 DISCUSSION

To sum up, the results show that the CSST spectroscopic survey is capable of delivering stellar radial velocities to a precision of $2-4\,\mathrm{km\,s^{-1}}$ for AFGKM types of stars at SNR = 100. The precision decreases to $4-15\,\mathrm{km\,s^{-1}}$

for hotter OB stars. The CSST spectroscopic survey aims to reach AB magnitude 5σ limit $\sim$21 mag per resolution element for point sources. It corresponds to about 17 mag at SNR = 100. It means that the CSST spectroscopic survey has a potential to provide reliable velocities for a huge number of stars for Galactic and stellar sciences, such as Galactic kinematics and searching for high-velocity stars and hyper-velocity stars (Brown 2015).

There are several simplifications in the current work. We ignored any systematic uncertainties in the CSS-OS data reduction process (such as sky subtraction and CCD charge transfer inefficiency correction). We did not consider variations of spectral resolution and SNRs as a function of wavelength either. We also ignored any uncertainties in the flux calibration processes. As mentioned in Section 3, it is highly possible to achieve a flux calibration precision of 1 per cent, using tens of

millions of stars as flux standards. Nevertheless, we can always use normalized spectra to derive stellar radial velocities, at a cost of slightly larger uncertainties.

Wavelength calibration plays an important role in the final precision of CSST radial velocities, in two ways. One is how precise the field-dependent dispersion solutions are, and the other is how precise the wavelength zero points are. With a new star-based method that can monitor and correct for possible errors in the CSST dispersion solutions using normal scientific observations of stars of known velocities, Yuan et al. (2021) have shown that it is possible to achieve a precision of a few $\mathrm{km\,s^{-1}}$ for the dispersion solutions. Here we discuss the precision of wavelength zero points δv_0, which depends on the precision of centroids of zero-order images $\Delta\mathrm{pixel}$.

It is known that $\Delta\mathrm{pixel}$ for a well-sampled stellar image can be written as $\Delta\mathrm{pixel} = \frac{1.335 \times \mathrm{FWHM}}{\mathrm{SNR}}$ (Lindegren 1978), where FWHM is in units of pixel. For the CSST spectrographs, the FWHM of their zero-order images is about 5.1 pixels (assuming a Gaussian profile) or smaller, given that the radius of 80% energy concentration of zero-order images is no larger than 0.3 arc-second and the sampling is 0.074 arc-seconds per pixel. For a 17 mag star that has a typical spectral SNR of 100, it can be easily estimated that the SNRs of its zero-order images (dominated by Poisson noise) of GU/GV/GI bands are larger than 500, assuming a 5% efficiency for the zero-order images and 20%, 40% and 40% efficiency for the GU, GV and GI band spectra (Zhan 2018). Therefore, $\Delta\mathrm{pixel}$ can be directly determined to a precision about 0.01 pixel, corresponding to a δv_0 precision of about $4\,\mathrm{km\,s^{-1}}$.

Given the fact that almost all CSST stellar targets will have very accurate positions and proper motions thanks to the Gaia mission (Lindegren et al. 2018), $\Delta\mathrm{pixel}$ can also be estimated indirectly from a star's sky position. For a 17 mag star, Gaia DR5 will deliver positions accurate to about 0.05 mas and proper motion accurate to about $0.04\,\mathrm{mas\,yr^{-1}}$ [1]. Assuming a typical epoch difference of 10 years between the Gaia DR5 and the CSST, the star will have a predicted position accurate to about 0.4 mas, corresponding to $\Delta\mathrm{pixel}$ value of about 0.005 and a δv_0 precision of about $2\,\mathrm{km\,s^{-1}}$. Note that we ignore errors in the astrometric solutions, which are supposed to be very small considering that a large number stars can be used. The above analyses show that possible velocity errors caused by wavelength zero points are comparable or smaller than Δv in our main results. The conclusion also holds for fainter stars.

In addition, we assumed perfect template spectrum for a given target in our simulation. To investigate possible effect of an imperfect template on velocity measurements, for each normalized spectrum, we have first tried every spectrum from the NGSL library rather than itself to find its closest spectrum as template to measure radial velocities, the results are shown in Figure 4 (lower-left panel), Figure 5 (right panel) and Figure 6 (lower-left panel). The uncertainties for most stars are almost the same to those using itself as template. The uncertainties are significantly larger for only few hot stars, due to lack of enough hot stars in the NGSL library. To further investigate additional uncertainties caused by an imperfect template, we used a G2-type star (HD095241) as an example. We compared velocity uncertainties using itself as the template with those using stars of different stellar parameters. Two stars (BD + 381670 and HD022484) were used. The T_{eff} differences are 243 K and 94 K, and the [Fe/H] differences are 0.23 and 0.24 dex, respectively. It was found that velocity uncertainties with the imperfect template are only larger by about 10%. The results suggest that the precision of velocities measurements is not sensitive to possible systematics in the templates.

The discussions above indicate that precision values obtained in the current work are upper limits. Many realistic situations have not been taken into account, such as lower SNRs, not clean background subtraction, overlapping (not only on spectra but also on zero-order images), no detected zero-order image, asymmetric and variable point spread function, charge transfer inefficiency etc. It is still unclear to what extent these complicated situations would affect the precision of the RV measured from slitless spectra. More investigations should be done with more dedicated simulated spectra considering all those situations in future works.

In the end, all targets in the NGSL are normal stars. However, the CSS-OS will observe various types of abnormal stars, such as emission line stars (young stellar objects, Ae stars, Be stars, cataclysmic variables) and white dwarfs. Due to the existence of strong emission lines or intrinsically very broad absorption features, the CSS-OS slitless spectra are very suitable to measure their velocities.

6 SUMMARY

By using the degraded NGSL spectra to stimulate the CSST stellar spectra, we have determined the best precision of CSST radial velocities, and its variations as functions of stellar parameters. We find that the best precision depends strongly on temperature, weakly on metallicity for only solar-like stars, and hardly on surface gravity. At SNR=100, the best precision is about $2 - 4\,\mathrm{km\,s^{-1}}$ for AFGKM stars, and $4 - 15\,\mathrm{km\,s^{-1}}$

---

[1] *https://www.cosmos.esa.int/web/gaia/sp-figure2*

for OB stars. The uncertainties of velocity measurement brought by wavelength calibration are considered, and are estimated to be around a few $\mathrm{km\,s^{-1}}$.

Velocity uncertainties using single GU/GV/GI band spectra are also explored. At the same SNR, the GU band performs the best, the GV band the second best, and then the GI band. The effects of spectral normalization and imperfect template on velocity measurements are investigated, and found to be weak if done properly. Given the precision of radial velocities and the large number of stars that can be observed, the CSST spectroscopic survey can enable interesting science such as searching for high-velocity stars and hyper-velocity stars.

We have made several simplifications that the results in the work are the upper limits of the real cases. To make the numbers come true, lots of effort is required to achieve accurate wavelength calibration, particularly in the GU band. In future we will re-visit the precision of velocity measurements using more realistic simulated CSS-OS data when available and extend to other stellar parameters, including temperature, metallicity, surface gravity, alpha and other elemental abundances.

References

Baranne, A., Queloz, D., Mayor, M., et al. 1996, A&AS, 119, 373

Brown, W. R. 2015, Annual Review of Astronomy and Astrophysics, 53, 15

Cao, Y., Gong, Y., Meng, X.-M., et al. 2018, MNRAS, 480, 2178

Glazebrook, K., Baldry, I., Moos, W., Kruk, J., & McCandliss, S. 2005, New Astronomy Reviews, 49, 374

Gong, Y., Liu, X., Cao, Y., et al. 2019, ApJ, 883, 203

Heap, S. R., & Lindler, D. J. 2007, Astronomical Society of the Pacific Conference Series, 374, Hubble's Next Generation Spectral Library (NGSL), eds. A. Vallenari, R. Tantalo, L. Portinari, & A. Moretti, 409

Irfan, M. O., Bobin, J., Miville-Deschînes, M.-A., & Grenier, I. 2019, A&A, 623, A21

Koleva, M., & Vazdekis, A. V. 2012, A&A, 538, A143,

Lindegren, L. 1978, in IAU Colloq. 48: Modern Astrometry, 197

Lindegren, L., Hernández, J., Bombrun, A., et al. 2018, A&A, 616, A2

Planck Collaboration, Abergel, A., Ade, P. A. R., et al. 2014, A&A, 571, A11

Schlegel, D., Finkbeiner, D., & Davis, M. 1998, Wide Field Surveys in Cosmology, 14, 297

Ting, Y.-S., Conroy, C., Rix, H.-W., & Cargile, P. 2017, ApJ, 843, 32

Yuan, H.-B., Deng, D.-S., & Sun, Y. 2021, RAA (Research in Astronomy and Astrophysics), 21, 74

Zhan, H. 2011, SCIENTIA SINICA Physica, Mechanica & Astronomica, 41, 1441

Zhan, H. 2018, in 42nd COSPAR Scientific Assembly, 42, E1.16